

行政院國家科學委員會專題研究計畫 成果報告

探討白梨蘆醇 Resveratrol 減緩骨質疏鬆症之機制:骨形蛋白-2 之角色及調控機轉
研究成果報告(精簡版)

計畫類別：個別型
計畫編號：NSC 95-2314-B-002-281-
執行期間：95年08月01日至96年07月31日
執行單位：國立臺灣大學醫學院一般醫學科

計畫主持人：嚴孟祿
共同主持人：郭明良
計畫參與人員：碩士班研究生-兼任助理：邱勤、胡欣怡

處理方式：本計畫可公開查詢

中華民國 96年11月01日

Forkhead Proteins Are Critical for Bone Morphogenetic Protein-2 Regulation and Anti-tumor Activity of Resveratrol^{*S}

Received for publication, March 22, 2007, and in revised form, May 14, 2007. Published, JBC Papers in Press, May 18, 2007, DOI 10.1074/jbc.M702452200

Jen-Liang Su^{†S¶1}, Ching-Yao Yang^{||**1}, Ming Zhao^{‡‡}, Min-Liang Kuo^{§§}, and Men-Luh Yen^{¶¶1||2}

From the [†]Graduate Institute of Cancer Biology, College of Medicine, China Medical University, Taichung 404, Taiwan, the ^SCenter for Molecular Medicine, China Medical University Hospital, Taichung 404, Taiwan, the [¶]Department of Biotechnology and Bioinformatics, Asia University, Taichung 41354, Taiwan, the ^{||}Department of Surgery, National Taiwan University Hospital, Taipei 100, Taiwan, the ^{**}Department of Traumatology, National Taiwan University Hospital, Taipei 100, Taiwan, the ^{‡‡}Vanderbilt Center for Bone Biology, Division of Clinical Pharmacology, Department of Medicine, Vanderbilt University, Nashville, Tennessee 37232-0575, the ^{§§}Institute of Toxicology, College of Medicine, National Taiwan University, Taipei 100, Taiwan, the ^{¶¶}Department of Primary Care Medicine, National Taiwan University Hospital, College of Medicine, No. 7, Chung Shan S. Rd., Taipei 100, Taiwan, and the ^{||}Department of Obstetrics and Gynecology, National Taiwan University Hospital, Taipei 100, Taiwan

Osteoporosis is a major public health problem and the most obvious preventive strategy, hormone replacement therapy, has lost favor due to recent findings of the Women's Health Initiative regarding increased risks of breast cancer and cardiovascular disease. Resveratrol, a naturally occurring compound possessing estrogenic activity, is thought to have considerable potential for therapy of osteoporosis. In the present study, resveratrol was found to exhibit bone-protective effects equivalent to those exerted by hormone replacement therapy and decrease the risk of breast cancer in the *in vivo* and *in vitro* models. Forkhead proteins were found to be essential for both effects of resveratrol. The bone-protective effect was attributable to induction of bone morphogenetic protein-2 through Src kinase-dependent estrogen receptor activation and FOXA1 is required for resveratrol-induced estrogen receptor-dependent bone morphogenetic protein-2 expression. The tumor-suppressive effects of resveratrol were the consequence of Akt inactivation-mediated FOXO3a nuclear accumulation and activation. Resveratrol is therefore anticipated to be highly effective in management of postmenopausal osteoporosis without an increased risk of breast cancer.

Osteoporosis is a major public health concern and is especially troublesome for menopausal and postmenopausal

females who suffer from estrogen deficiency. It is widely believed that osteoporosis results from imbalance between bone resorption and bone formation leading to net bone loss (1). However, hormone replacement therapy has lost favor due to the Women's Health Initiative finding that extended hormone replacement therapy increases the risks of both breast cancer and cardiovascular disease (2). The current challenge in prevention or therapy of osteoporosis, therefore, is to identify treatments that share the protective effects of estrogen but lack its side effects. Certain natural dietary substances may act to minimize bone loss in postmenopausal women. The phytoestrogens, therefore, are potentially important in the prevention of postmenopausal osteoporosis caused by estrogen deficiency.

Resveratrol is a polyphenolic phytoalexin compound found in various plants and has been characterized as a phytoestrogen based on its ability to bind to and activate estrogen receptor (ER)³ (3). As a potential antioxidant, resveratrol has been reported to exhibit a wide range of biological and pharmacological properties, including 1) cancer-chemopreventive potential by blocking carcinogenesis at various stages; 2) cardiovascular protection by promoting nitric oxide production, inhibiting platelet aggregation and inflammation, and reducing toxic cholesterol level; and 3) anti-aging potential demonstrated by the effect of increasing the lifespan of yeast and flies. The mechanism studies have indicated that resveratrol acts at multiple levels, such as cellular signaling, enzymatic pathways, apoptosis, and gene expression (4–10). Recent studies have shown that resveratrol stimulates osteoblast differentiation and has a marked effect in reducing loss of bone mass in ovariectomized (OVX) rat model (6, 11, 12), indicating that resveratrol could be a preventive or therapeutic agent for osteoporosis. Details

* This work was supported by National Science Council, Taiwan (Grants NSC 94-2314-B-002-212, NSC 95-2314-B-002-281, NSC 95-2314-B-002-110-MY3, and NSC 96-2320-B-039-004-MY2) and by the Ministry of Economic Affairs, Taipei, Taiwan (Grant 93-EC-17-A-19-S1-0016). The Luciferase expression plasmids under the control of the BMP-2 promoter (pBMP-2-Luc) were kindly provided by G. R. Mundy (Medicine, Pharmacology, Orthopedics, Cancer Biology, Vanderbilt Center for Bone Biology, Vanderbilt University Medical Center). The authors have declared that no conflict of interest exists. The costs of publication of this article were defrayed in part by the payment of page charges. This article must therefore be hereby marked "advertisement" in accordance with 18 U.S.C. Section 1734 solely to indicate this fact.

^S The on-line version of this article (available at <http://www.jbc.org>) contains supplemental Figs. S1 and S2 and Table S1.

¹ Both authors contributed equally to this work.

² To whom correspondence should be addressed (present address): Dept. of Primary Care Medicine, National Taiwan University Hospital and National Taiwan University, College of Medicine, No. 7, Chung Shan S. Rd., Taipei, Taiwan. Tel.: 886-2-23123456 (ext. 5122); Fax: 886-2-2391-1302; E-mail: ntu88447004.tw@yahoo.com.tw.

³ The abbreviations used are: ER, estrogen receptor; BMP-2, bone morphogenetic protein-2; OVX, ovariectomized; primary OBs, primary cultured osteoblast cells; ALP, alkaline phosphatase; BMD, bone mineral density; TNF α , tumor necrosis factor α ; E₂, 17 β -estradiol; ERE, ER response element; ChIP, chromatin immunoprecipitation; siRNA, short interfering RNA; ER α -binding probe, non-radiolabeled probe; FRE, FOXO-responsive elements; SIR, silent information regulator; IKK, I κ B kinase; siRNA, short interference RNA; ELISA, enzyme-linked immunosorbent assay; RT, reverse transcription; TRITC, tetramethylrhodamine isothiocyanate.

Forkhead Is Critical for BMP-2 and Tumor Suppression

regarding the mechanisms through which resveratrol exerts its bone protection and tumor suppression are lacking. Therefore, identifying the molecular mechanisms of action is essential for understanding both the beneficial and adverse effects of resveratrol.

Although the mechanisms of osteoporosis are not entirely clear, they are likely relate to decreased availability or effects of bone growth factors, such as bone morphogenetic proteins (BMPs). BMPs, structurally related to the transforming growth factor- β superfamily, were originally identified by their capacity to induce ectopic bone formation in rodents (13). Among BMP family members, BMP-2 has been extensively studied and demonstrated to play a crucial role in inducing osteoblast differentiation and bone formation during embryonic skeletal development and postnatal bone remodeling (14, 15). Skeletal aging studies have shown that both anabolic activity and gene expression of *BMP-2* are decreased in the senile animals with osteopenia, suggesting that the decay of BMP-2 function may account for one of the molecular pathogenic mechanisms of osteoporosis (16, 17). A recent study has found a linkage of osteoporosis to specific polymorphisms in the *BMP-2* gene, implicating that *BMP-2* is an osteoporosis-associated gene (18).

Findings of the present study reveal that resveratrol not only shares the bone-protective effects of hormone replacement therapy but also decreases the risk of occurrence of breast cancer. We found the forkhead protein, FOXA1, was involved in resveratrol-induced ER-dependent BMP-2 expression. Our findings also show that Akt inactivation-mediated FOXO3a nuclear accumulation and activity are required for the tumor suppressive effect of resveratrol. Forkhead proteins play a significant role in both resveratrol-mediated bone protective function and breast cancer suppression. We provide evidence that resveratrol would be a critical therapeutic strategy for prevention of osteoporosis.

EXPERIMENTAL PROCEDURES

Antibodies and Reagents—Anti-BMP-2 antibody, anti- β -actin antibody, BMP-2 ELISA kit, osteopontin ELISA kit, and noggin were obtained from R&D Systems (Minneapolis, MN). The osteocalcin ELISA kit was obtained from Biocompare Inc. (San Francisco, CA). Fetal bovine serum, glutamine, and penicillin/streptomycin were purchased from HyClone (Logan, UT). Anti-p-Akt antibody, anti-Akt antibody, anti-p-Src antibody, anti-Src antibody, anti-ER α antibody, anti-ER β antibody, anti-PCNA antibody, anti-c-Jun antibody, anti-c-Fos antibody, anti-Sp1 antibody, secondary antibodies, and protein G plus-agarose were all purchased from Santa Cruz Biotechnology (Santa Cruz, CA). For the siRNA studies, a smart pool of double-stranded siRNA against ER α or nonspecific siRNA were obtained from Dharmacon Tech (Lafayette, CO) and used according to the manufacturer's instructions. *trans*-Resveratrol was obtained from Sigma. Tamoxifen and PP2 were purchased from Calbiochem Novabiochem Co.

Cell Culture—The human osteoblast-like cell line MG-63 and MC3T3-E1 mouse clonal osteogenic cells were purchased from American Type Culture Collection (Manassas, VA). Cells were cultured in minimal essential medium supplemented with 10% fetal bovine serum and antibiotics (100 IU/ml penicillin G

and 100 μ g/ml streptomycin). Cell cultures were maintained at 37 °C in a humidified 5% CO₂ atmosphere. For the cell cycle analysis, proliferating cells were serum-starved for 24 h and then treated with vehicle or resveratrol for 24 h. Cells were then subjected to flow cytometric analysis as described previously (19).

Establishment of Stable Transfectants—MC3T3-E1 cells were transfected with pcDNA3 containing the dominant negative mutant Src, which were kindly provide by Dr. Ruey-Hwa Chen (Dept. of Molecular Medicine, College of Medicine, National Taiwan University, Taipei, Taiwan), or with the empty vector using Lipofectamine Plus reagent (Invitrogen). After 48 h, stably transfected cells were selected by media containing 600 μ g/ml G418 for 4 weeks. Pools of six clones of MC3T3-E1/DN-Src or MC3T3-E1/vector were isolated for further studies. MDA-MB-231 cells were cotransfected with specific siRNA against FOXO3a cloned into pSuper vector and pcDNA3 in 10:1 ratio, which were kindly provide by Dr. Alex Toker (Dept. of Pathology, Beth Israel Deaconess Medical Center, Harvard Medical School). After 48 h, stably transfected cells were selected by media containing 800 μ g/ml G418 for 4 weeks. Pools of 10 clones of MDA-MB-231/siFOXO3a or MDA-MB-231/siControl were isolated for further studies.

BMD by DEXA—Female Wistar rats were sham-operated or OVX. BMD was measured in anesthetized rats (87 mg/kg ketamine and 13 mg/kg xylazine) after treated with various concentrations of resveratrol by orally feeding them every 2 days for 10 weeks using DEXA (QDR 4500a, Hologic, Inc.). Small animal software (Hologic, Inc.) was used to obtain BMD in the femur/tibia. The femur/tibia site consisted of the proximal half of the tibia and the entire femur. All animal work was performed in accordance with protocols approved by the Institutional Animal Care and Use Committee of the College of Medicine, National Taiwan University. Animals were maintained in accordance with the National Institutes of Health Guide for the Care and Use of Laboratory Animals.

Anchorage-independent Growth Assay—Colony-forming assays in soft agarose were performed as described previously (19). Cells were seeded in 6-well culture dishes in suspensions of 0.35% Agar noble in Dulbecco's modified Eagle's medium supplemented with 10% fetal bovine serum on top of a bed of 0.7% Agar noble in the same complete medium. After 3 weeks, tumor cell colonies measuring at least 50 μ m were counted from six replicates per treatment under a dissecting microscope.

Assaying the Levels of Osteocalcin, Osteopontin, and BMP-2—Osteocalcin, osteopontin, and BMP-2 ELISA kits were used to detect osteocalcin, osteopontin, and BMP-2 levels, respectively. Briefly, cells were treated with various concentrations of resveratrol for the indicated times. The culture medium was collected and measured for osteocalcin, osteopontin, and BMP-2, respectively. These samples were placed in 96-well microtiter plates coated with monoclonal-detective antibodies and incubated for 2 h at room temperature. After removing unbound material by washing with washing buffer (50 mM Tris, 200 mM NaCl, and 0.2% Tween 20), horseradish peroxidase-conjugated streptavidin was added to bind to the antibodies. Horseradish peroxidase cat-

alyzed the conversion of a chromogenic substrate (tetramethylbenzidine) to a colored solution, with color intensity proportional to the amount of protein present in the sample. The absorbance of each well was measured at 450 nm. Results are presented as the percentage of change of the activity compared with the untreated control.

cDNA Array Analysis—The GEArray Q series of Mouse Osteogenesis Gene Arrays from SuperArray Bioscience are application-specific cDNA arrays. GEArray Q series Mouse Osteogenesis Gene Array is designed to profile gene expression in the process of osteogenic differentiation. The genes regulating this process include growth factors and their internal cell signaling molecules, as well as the early and later differentiation genes. We used this Mouse Osteogenesis Gene Array to determine simultaneously the expression profile of the genes involved in the regulation of osteogenic differentiation. Experimental procedures and analyses were performed according to the manufacturer's instructions.

Immunoprecipitation and Western Blot Analysis—Protein expression was detected by Western blot analysis as described previously (19). Equal amounts of protein were incubated with specific antibody immobilized onto protein A-Sepharose for 2 h at 4 °C with gentle rotation. Beads were washed extensively with lysis buffer, boiled, and microcentrifuged. Proteins were resolved on SDS-PAGE and transferred to nitrocellulose membrane. After blocking, blots were incubated with specific primary antibodies. After washing and incubating with secondary antibodies, immunoreactive proteins were visualized by the ECL detection system (Amersham Biosciences). Where indicated, the membranes were stripped and reprobed with another antibody.

RNA Isolation and Reverse Transcriptase-PCR—Total RNA was isolated using RNAzol B and reverse transcribed into single-stranded cDNA with Moloney murine leukemia virus reverse transcriptase and random hexamers (Promega) according to the manufacturer's instructions. The primer sequences for osteocalcin were: 5'-ATGAGGACCCTCTCTCTGCTC-3' (forward) and 5'-CTAACGGTGGTGCCATAGAT-3' (reverse); for osteopontin were: 5'-ATGAGACTGGCAGTGGTT-3' (forward) and 5'-GCTTTCATTGGAGTTGCT-3' (reverse). The primer sequences for BMPs were designed as described previously (20). The reaction mixture was first denatured at 95 °C for 10 min. The PCR condition was 95 °C for 1 min, 52 °C for 1 min, and 72 °C for 1 min for 30 cycles, followed by 72 °C for 10 min. PCR products were visualized by ethidium bromide staining after agarose gel electrophoresis. The PCR results were repeated at least twice from a particular cDNA sample, and from at least two independent cDNA preparations.

BMP-2 Promoter-luciferase Reporter Construction and Reporter Assay—The luciferase expression plasmids under the control of the BMP-2 promoter (pBMP-2-Luc) were kindly provided by Mundy G. R. (University of Texas Health Science Center at San Antonio, San Antonio, TX). To construct a plasmid containing the ERE or Sp1 site mutations in pBMP-2-Luc, we used pBMP-2-Luc promoter as a template and designed a mutated ERE site (pBMP-2-LucmERE, GGCCACTCTGACC to AACCACTCTACCT) or a mutated Sp1 site (pBMP-2-Luc-

mSp1, CGGCCCGCCCGCC to CTTCCCTTCCGCC) by using the QuikChange® site-directed mutagenesis kit (Stratagene). The luciferase assays were carried out using the Dual-Luciferase® reporter assay kit (Promega) according to protocols provided by the manufacturer.

Chromatin Immunoprecipitation Assay—Cells were fixed with 1% formaldehyde, washed, and lysed. The nuclei were released by processing in a Dounce homogenizer followed by lysis in 100–200 μ l of nucleus lysis buffer (50 mM Tris-HCl (pH 8.0), 10 mM EDTA, and 1% SDS). One microgram of antibody was added to 0.5–1.0 ml of the lysate and rotated overnight at 4 °C. The immunocomplexes were then pulled down by using protein G-conjugated magnetic Dynabeads (DynaL Biotech), and the bound protein was eluted twice with 30 μ l of 0.1 M citrate buffer (pH 3.0). The reverted DNA was purified with a Miniprep spin column (Qiagen) and then eluted in 50 μ l of 10 mM Tris-HCl (pH 8.0). The BMP-2 promoter region was amplified by conventional PCR with primers 5'-GGGTTGGAACCTCCAGACTGT-3' (forward) and 5'-GAAGAGTGAGTGGACCCCAG-3' (reverse). The PCR program was 95 °C for 10 min followed by 35 cycles at 95 °C for 45 s, 52 °C for 1 min, and 72 °C for 1 min. Input DNA and DNA recovered after immunoprecipitation were quantified using PicoGreen fluorescence (Molecular Probes, Eugene, OR). Equivalent masses of immunoprecipitation and input DNA were compared by real-time PCR as described above for RT-PCR with the following modifications. *Taq* polymerase was from Qiagen (Hot Start), and cycling conditions were 95 °C for 15 min followed by 45 cycles of 94 °C for 20 s, 61 °C for 1 min, and 72 °C for 40 s. Data are presented as the ratio of immunoprecipitation to input C_t values.

siRNA—A 21-bp siRNA was designed against the FoxA1 transcript and synthesized by Dharmacon and transfected using Lipofectamine 2000 (Invitrogen) as described previously (21). FOXO3a-siRNA (5'-GAGCUCUUGGUGGAUCAU-CTT-3') duplex (Dharmacon, 4 μ M/2 \times 10⁶ cells) was transfected by Lipofectamine 2000 (Invitrogen), and lysates were prepared 48 h after transfection as described previously (22).

Immunofluorescence Staining—Detection of protein expression by immunofluorescence staining was described previously (19). Briefly, cells were fixed in 3% paraformaldehyde and then blocked by incubation in 2.5% bovine serum albumin in phosphate-buffered saline. Primary antibodies as indicated were applied to the slides at a dilution of 1:50 and incubated at 4 °C overnight. The samples were treated with fluorescein isothiocyanate-conjugated or TRITC-conjugated secondary antibody (Sigma). The fluorescein isothiocyanate-labeled or TRITC-labeled cells were then analyzed by fluorescence microscopy.

Orthotropic Breast Tumor Growth Assay—6-week-old female SCID mice were supplied by the animal center of the College of Medicine, National Taiwan University, Taipei, Taiwan. Mice were orthotropic inoculated with tumor cells into the mammary fat pad as described previously (22). Tumor development was followed in individual animals (eight per group) by measuring tumor length (*L*) and width (*W*) with calipers every 3 days. Tumor volume was calculated with the formula, $LW^2/2$. All animal work was performed in accordance

Forkhead Is Critical for BMP-2 and Tumor Suppression

with protocols approved by the Institutional Animal Care and Use Committee of the College of Medicine, National Taiwan University.

Fractionations of Cells and Electrophoretic Mobility Shift Assay—Nuclear extracts were prepared as described previously (22). Electrophoretic mobility shift assay for DNA binding in MC3T3-E1 cells was performed using the probe purchased from Santa Cruz Biotechnology and [α - 32 P]dCTP end-labeled in a 20- μ l reaction mixture for 20 min at room temperature. For competition experiments, a 5-fold excess of unlabeled oligonucleotide was added to the binding reactions. The reaction products were analyzed by 5% nondenaturing PAGE using Tris (12.5 mM), boric acid (12.5 mM), and EDTA (0.25 mM), pH 8.3, for a period of 4–5 h at 280–300 V and 10–12 mA. The gels were then dried and exposed, for an appropriate time period, to AmershamTM film (Amersham Biosciences) at -70°C while using an intensifying screen.

Quantification of Apoptotic Osteoblasts in Undecalcified Bone Sections—Four-month-old female Wistar rats were subjected to a sham operation or to ovariectomy. Lumbar vertebrae (L1 to L5) were removed from female rats after 10 weeks. Apoptotic osteoblasts were detected in undecalcified plastic-embedded sections by terminal deoxynucleotidyl transferase-mediated dUTP nick end labeling using the Klenow FragEL detection kit (Oncogene) according to the manufacturer's instruction.

Alkaline Phosphatase Activity Assay—Triplicate aliquots of 0.1% SDS cell lysates were used for biochemical evaluation of ALP activity using the Sigma-Aldrich kit number 104, according to the manufacturer's instruction.

In Vitro Quantification of Apoptosis by Flow Cytometry—Cells were harvested and washed with phosphate-buffered saline, and hypodiploid cells were analyzed by flow cytometry as described previously (Su *et al.* 19). Briefly, cells were washed with phosphate-buffered saline and re-suspended in 500 μ l of a buffer (0.5% Triton X-100/phosphate-buffered saline/0.05% RNase A) and incubated for 30 min. Then, 0.5 ml of propidium iodide solution (50 μ g/ml) was added. Cells were then left on ice for 15–30 min. Fluorescence emitted from propidium iodide-DNA complexes was quantified after laser excitation of the fluorescent dye by fluorescence-activated cell sorting flow cytometry (BD Biosciences). Finally, the extent of apoptosis was determined by measuring DNA content of the cells below the G_0/G_1 peak.

Real-time Quantitative RT-PCR—Real-time PCR was performed using a Roche LightCycler according to the manufacturer's protocol (Roche Applied Science). After reverse transcription reaction (20 μ l) using 2 μ g of total RNA, real-time PCR was carried out in a 20- μ l final volume using the LightCycler-FastStart DNA Master SYBR Green I kit (Roche Applied Science). The reaction mix contained 1 \times LightCycler-FastStart Master SYBR Green I, 0.5 μ M of each primer, 4 mM MgCl_2 , and 2 μ l of cDNA from (20 μ l of) reverse transcription reaction. The conditions of the real-time PCR were as described previously (23). Fluorescence was measured at 82°C for 5 s.

RESULTS

Resveratrol Increases Osteogenic Responses and Prevents Ovariectomy-induced Bone Loss—To examine the effects of resveratrol on proliferation and differentiation of osteoblastic cells, MC3T3-E1, MG63, and rat primary cultured osteoblast cells (primary OBs) were treated with various concentrations of resveratrol, and the fraction of cells in S-phase was determined. Treatment with resveratrol at the concentrations indicated in Fig. 1A significantly increased the proliferation of MC3T3-E1 and MG63 cells, closely matching the increase observed in primary OBs cultured under identical conditions. Biochemical analysis of the osteoblast differentiation marker, ALP, confirmed that enzyme activity increased in confluent preparations of these cells after treatment with resveratrol for 7 days (Fig. 1B). Expression of the osteoblast differentiation markers, osteocalcin and osteopontin, was measured by RT-PCR and ELISA assay. Resveratrol increased expression of both osteocalcin and osteopontin at the mRNA and protein levels in all three cell lines (Fig. 1C). The bone protective activity of resveratrol was also examined in ovariectomized mice. Resveratrol preserved both bone mineral density (BMD) and serum ALP activity in ovariectomized, but not sham-operated mice, and preservations were dose-dependent and significant (Fig. 1D). In addition, treatment with 10 mg/kg resveratrol restored BMD and serum ALP activity in ovariectomized mice to degrees observed in sham controls and as effectively as estradiol (Fig. 1D). To explore the anti-apoptotic effects of resveratrol in osteoblasts, MC3T3-E1 cells and primary OBs were subjected to pro-apoptotic stimuli in the absence or presence of resveratrol. The phytoestrogen prevented induction of apoptosis in MC3T3-E1 cells and primary OBs in response to etoposide or $\text{TNF}\alpha$ (Fig. 1E). Ovariectomy increased vertebral osteoblast apoptosis by 4.2-fold, compared with sham-operated controls (Fig. 1F). The osteoblast apoptosis was prevented in ovariectomized mice receiving either resveratrol or 17β -estradiol (Fig. 1F). These *in vitro* and *in vivo* findings support the potency and efficacy of resveratrol for prevention of both bone loss and osteoblast apoptosis.

Resveratrol Prevents Breast Cancer Progression—To test the possibility that resveratrol increases the risk of breast cancer, effects of the drug on breast tumor growth were investigated. Estrogen-negative and estrogen-positive breast cancer cells were treated with vehicle, E_2 , or resveratrol and analyzed for extent of proliferation and anchorage-independent growth by DNA flow cytometry and the soft agar colony-forming assay, respectively. Treatment with resveratrol resulted in significant reductions in proliferation and anchorage-independent colony formation in the ER-positive (Fig. 2A) and ER-negative (Fig. 2B) breast cancer cells. In the orthotopic tumor growth assay, treatment with resveratrol reduced either E_2 -induced MCF-7 tumor growth or MDA-MB-231 tumor growth (Fig. 2C). In addition, the induction of tumor formation in response to treatment with E_2 was significantly decreased by resveratrol (100% *versus* 40%, respectively). Resveratrol also reduced tumor formation in MDA-MB-231-bearing mice (100% in vehicle and E_2 treatment group *versus* 85% in resveratrol treatment group). Tumor weight decreased by 54.6% in MCF-7-bearing mice

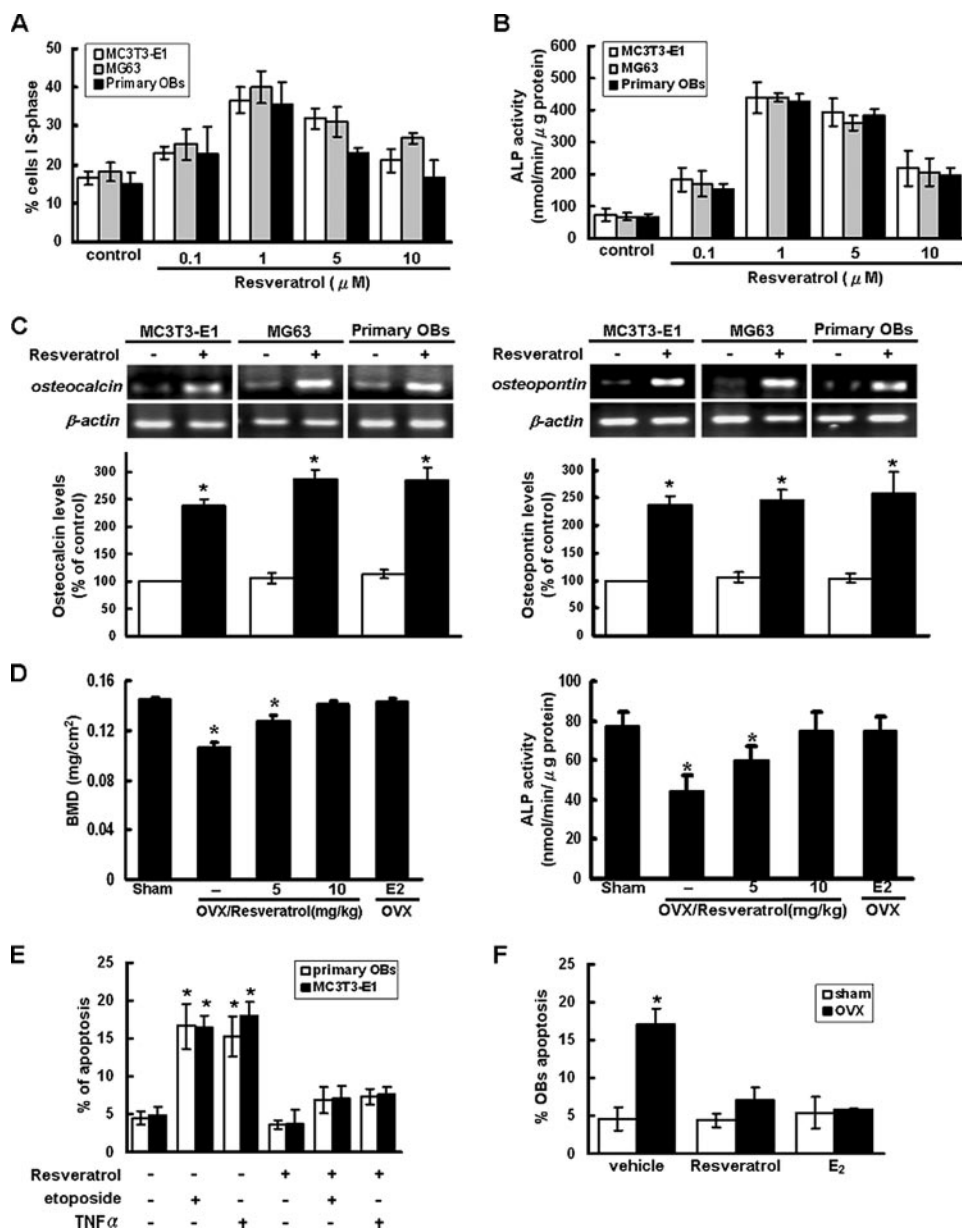


FIGURE 1. Resveratrol increases the osteogenic responses. *A*, stimulation of cell proliferation. The indicated cells were serum-starved for 48 h in the presence of resveratrol at the indicated concentrations. The percentage of cells in S phase was then determined by DNA flow cytometry. *B*, induction of alkaline phosphatase (ALP) activity. The indicated cells were treated at confluence with the indicated concentrations of resveratrol for 72 h. ALP activity was then measured with the Sigma-Aldrich kit number 104 according to the manufacturer's instructions. Findings represent treatments performed in three separate experiments. *C*, increased expression of osteocalcin and osteopontin. The indicated cells were treated with 1 μM resveratrol for 72 h. Expression of osteocalcin and osteopontin mRNA was determined by RT-PCR (upper panels). The amounts of osteocalcin and osteopontin in culture medium were determined with osteocalcin and osteopontin ELISA kits (lower panels). *D*, increased bone mineral density (BMD) and ALP activity *in vivo*. Female Wistar rats were given a sham operation or were ovariectomized (OVX). Rats that underwent OVX were treated with the indicated concentrations of resveratrol by oral feeding. Femur/tibia BMD and serum ALP activities were determined 10 weeks after surgery. Bars represent means ± S.D. of *n* = 8 mice/group. Asterisks denote a statistically significant difference compared with values for the sham-operated group (*, *p* < 0.05). *E*, anti-apoptotic effects. Osteoblasts were treated with the indicated pro-apoptotic stimuli in the presence or absence of resveratrol for 24 h, followed by quantification of apoptosis. Measurements were conducted in triplicate, and representative findings are presented. Findings were reproduced on three separate occasions. Bars represent means ± S.D. Asterisks denote a statistically significant difference compared with values for untreated control (*, *p* < 0.05). *F*, anti-apoptotic effects *in vivo*. Sham-operated and OVX rats were treated with vehicle, resveratrol (10 mg/kg), or E₂ (0.1 mg/kg). Ten weeks later, osteoblast apoptosis was determined in sections of L1 through L4 vertebrae. Bars indicate means ± S.D. *, *p* < 0.05 versus the sham-operated group.

mice treated with resveratrol as compared with the vehicle-treated group (194 ± 57 mg versus 344 ± 43 mg, respectively). Findings from these two experiments are summarized in Table 1. Resveratrol is therefore concluded to inhibit the induction and growth of breast cancer cells.

Resveratrol Induces BMP-2-dependent Osteoblast Differentiation—To study the downstream effector genes of the resveratrol-induced osteogenic response, non-biased cDNA array analysis involving cDNA sequences corresponding to functions related to regulation of osteogenic differentiation was performed. Under the highly stringent conditions used, the *BMP-2* gene was identified as one of the highly increased genes in resveratrol-treated, but not in vehicle-treated, primary OBs (supplemental Table S1). To substantiate this finding, expression of mRNAs for the BMPs in response to resveratrol was analyzed by RT-PCR. Treatment of primary OBs (Fig. 3A, left panel) or MC3T3-E1 cells (data not shown) with resveratrol resulted in a time-dependent increase in expression of the mRNA for *BMP-2*, but not of other BMP mRNAs. The RT-PCR findings therefore support the findings from the cDNA microarray analysis. The induction of *BMP-2* expression in response to resveratrol in human and murine osteoblast-like cell lines as well as in primary OBs was also observed using quantitative real-time RT-PCR analysis (Fig. 3A, right panel). As expected, treatment with resveratrol also increased *BMP-2* protein expression in a time- and dose-dependent manner as determined by Western blotting and *BMP-2* ELISA assay, respectively (Fig. 3B). Effects of resveratrol on *BMP-2* expression were also explored with the *in vivo* model. Serum concentrations of *BMP-2* were decreased by ovariectomy, and treatment with either E₂ or 10 mg/kg resveratrol restored the

treated with resveratrol as compared with mice treated with E₂ (134 ± 33 mg versus 295 ± 47 mg, respectively). Furthermore, tumor weight decreased by 43.6% in MDA-MB-231-bearing

BMP-2 concentrations to those of sham-operated controls (Fig. 3C). Resveratrol is therefore concluded to increase *BMP-2* expression *in vitro* and *in vivo*.

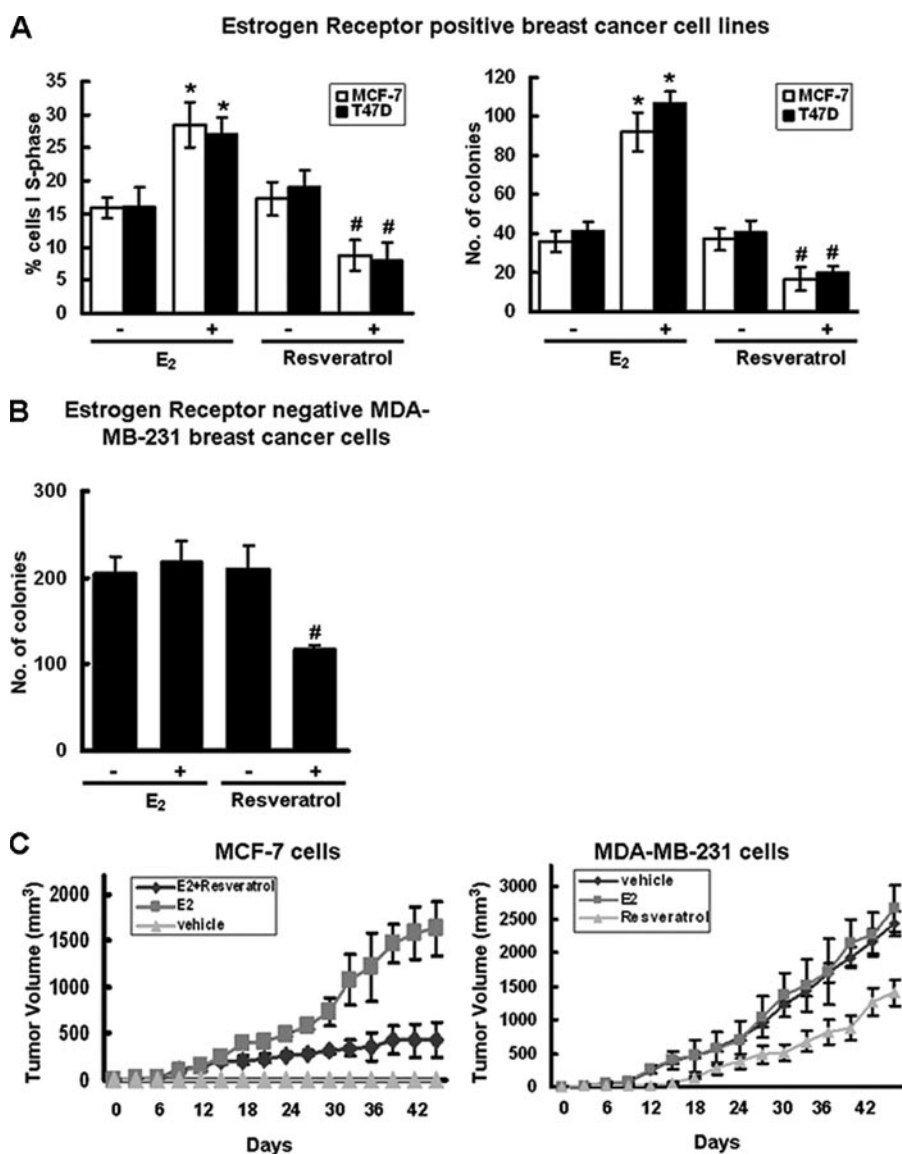


FIGURE 2. Resveratrol decreases breast tumor formation. A and B, proliferation and growth of estrogen-positive and estrogen-negative cells in response to E₂ or resveratrol. Two estrogen-positive cell lines, MCF-7 and T47D (A), and MDA-MB-231 estrogen-negative breast cancer cells (B) were treated with vehicle, E₂ (10 nM), or resveratrol (1 μM) and analyzed for extent of proliferation and anchorage-independent growth by DNA flow cytometry and the soft agar colony-forming assay, respectively. Bars indicate means ± S.D. Asterisks denote a statistically significant induction compared with values for the untreated control. #, significant reduction compared with values for the untreated control. Results represent findings of three separate experiments, and all incubations were conducted in triplicate. C, growth patterns of orthotopic xenograft tumors formed by MCF-7 cells or MDA-MB-231 cells in nude mice. Animals were treated with vehicle, E₂ (0.1 mg/kg/2days), or resveratrol (10 mg/kg/2 days). Each value represents the mean ± S.D. of eight primary tumors.

TABLE 1
Resveratrol decreases breast tumor formation in an orthotopic animal model

Cell line/treatment	Tumor formation		Tumor weight	
	Number of mice with tumors/total number of mice	p value	Mean ± S.D.	p value
MCF-7/vehicle	0/20		mg	
MCF-7/E ₂ plus vehicle	20/20		ND ^a	
MCF-7/E ₂ plus resveratrol	8/20	p < 0.01 ^b	134 ± 33	p < 0.01 ^b
MDA-MB-231/vehicle	20/20		344 ± 43	
MDA-MB-231/E ₂	20/20		359 ± 47	
MDA-MB-231/resveratrol	17/20	p < 0.05 ^c	194 ± 57	p < 0.01 ^c

^a ND, not detectable.

^b As compared with the MCF-7/E₂ group by one-way analysis of variance with post-hoc comparisons by least significant difference.

^c As compared with the MDA-MB-231/vehicle group by one-way analysis of variance with post-hoc comparisons by least significant difference.

To explore the hypothesis that induction of BMP-2 is required for resveratrol-induced osteogenic function, BMP-2 signaling in osteoblasts was blocked with a BMP-2-specific neutralizing antibody or with the antagonist, noggin. Treatment with BMP-2-specific neutralizing antibody, but not IgG control antibody, decreased resveratrol-induced ALP activity in MC3T3-E1 cells as well as in primary OBs cells in a dose-dependent manner (Fig. 3D, left panel). In addition, treatment of osteoblast cells with noggin notably diminished resveratrol-induced ALP activity (Fig. 3D, right panel). Treatment with either BMP-2-specific neutralizing antibody or noggin also abolished resveratrol-mediated anti-apoptotic activity in osteoblastic cells (Fig. 3E). Increased expression of BMP-2 is therefore concluded to be required for resveratrol-mediated osteogenic differentiation and for the anti-apoptotic effects of the drug in osteoblasts.

Src-mediated ER Signaling Pathway Is Required for Resveratrol-induced BMP-2 Expression—To explore the mechanism(s) through which regulation of BMP-2 expression participates in cellular responses to resveratrol, a series of BMP-2 promoter-reporter mutation constructs were employed. These constructs, which are presented in Fig. 4A, were designated pBMP2, pBMP2Δ1, pBMP2Δ2, pBMP2Δ3, pBMP2/mERE, and pBMP2/mSp1. Resveratrol significantly increased luciferase activity in pBMP2- and pBMP2Δ1-trans-

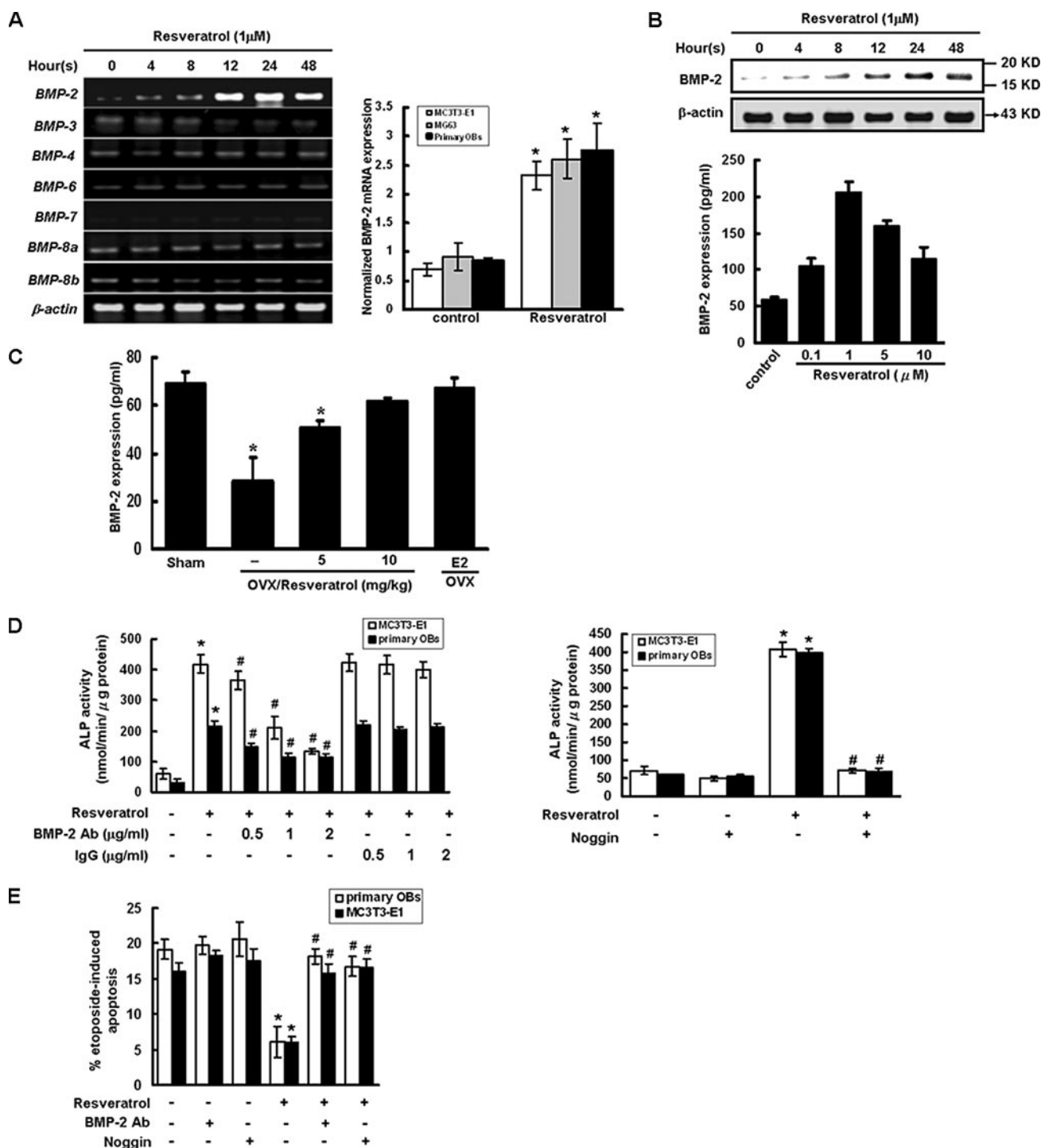


FIGURE 3. Resveratrol induces BMP-2-dependent osteoblast differentiation. *A*, expression of mRNAs for the BMPs. *Left panel*: primary osteoblasts (OBs) were treated with 1 μ M resveratrol for the indicated times, followed by measurements of expression of BMP mRNAs by RT-PCR. *Right panel*: the indicated cells were treated with 1 μ M resveratrol for 48 h. BMP-2 mRNA expression was measured by quantitative RT-PCR and normalized. *B*, BMP-2 protein expression. *Upper panel*: osteoblasts were treated with 1 μ M resveratrol for the indicated times, followed by measurements of BMP-2 expression by Western blotting. *Lower panel*: the amounts of BMP-2 in culture medium after 48 h of treatment at the indicated concentrations of resveratrol were measured using BMP-2 ELISA kits. *Bars* indicate means \pm S.D. of $n = 8$ mice/group. *Asterisks* denote a statistically significant difference compared with values for the sham-operated group (*, $p < 0.05$). *C*, BMP-2 protein expression *in vivo*. Ovariectomized (OVX) rats were treated with the indicated concentrations of resveratrol or with estrogen by oral feeding, and serum BMP-2 concentrations were determined with BMP-2 ELISA kits at 10 weeks after surgery. *Bars* represent means \pm S.D. of $n = 8$ mice/group. *Asterisks* denote a statistically significant difference compared with values for the untreated control (*, $p < 0.05$). *D*, BMP-2 and induction of alkaline phosphatase (ALP) activity. Primary osteoblasts and MC3T3-E1 cells were treated with the indicated concentrations of resveratrol and BMP-2 neutralizing or control antibody (*left*), or with and without 1 μ M resveratrol and/or 0.5 μ g/ml noggin (*right*) for 48 h, followed by measurements of ALP activity using the Sigma-Aldrich kit number 104. *Asterisks* denote a statistically significant difference compared with values for the untreated control (*, $p < 0.05$). Induction of activity was highly sensitive to inhibition by treatment with BMP-2 neutralizing antibody or noggin, as indicated by the # symbol. *E*, BMP-2 and the inhibition of etoposide-induced apoptosis. Primary osteoblasts and MC3T3-E1 cells were treated with 1 μ M resveratrol, 2 μ g/ml BMP-2 neutralizing antibody, and/or 0.5 μ g/ml noggin as indicated for 48 h, followed by determination of etoposide-induced apoptosis by measurement of the DNA content of cells below the G_0/G_1 peak. *Asterisks* denote a statistically significant difference compared with values for the untreated control (*, $p < 0.05$). The resveratrol-dependent reduction in apoptosis was overturned by treatment with BMP-2 neutralizing antibody or noggin to significant degrees, as indicated by the # symbol.

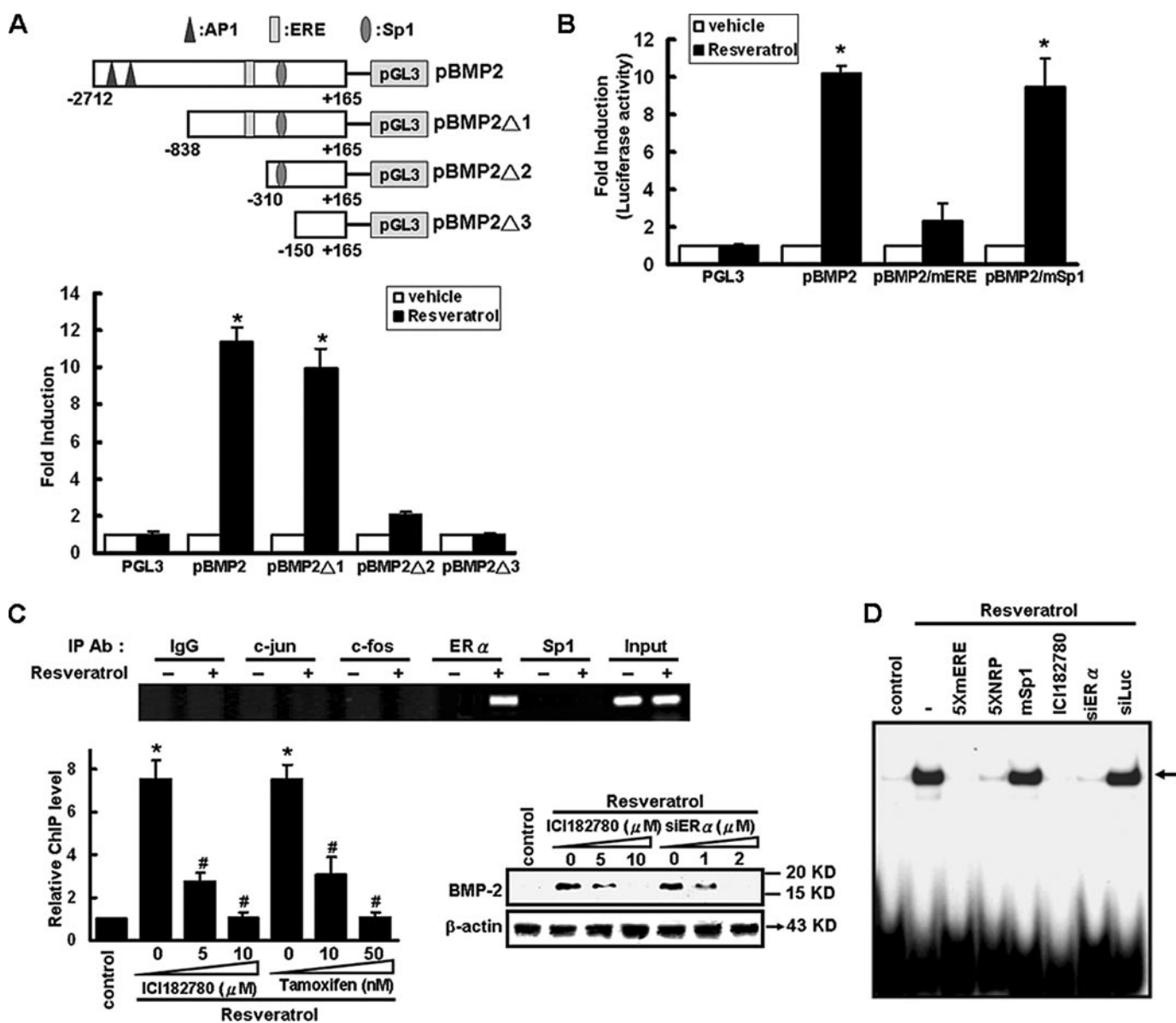


FIGURE 4. ER is involved in resveratrol-induced BMP-2 expression. *A* and *B*, MBP-2 constructs and resveratrol-stimulated BMP-2 promoter reporter activity. MC3T3-E1 cells transfected with various BMP-2 promoter-reporters were treated with 1 μ M resveratrol or vehicle for 4 h, followed by measurement of luciferase activity. Bars indicate means \pm S.D. *, $p < 0.05$ as compared with the vehicle-treated group. *C*, association of ER with the BMP-2 promoter in resveratrol-treated cells. MC3T3-E1 cells were treated with or without 1 μ M resveratrol, and then processed for a ChIP assay using various transcription factor antibodies. Relative levels of ER-DNA complex were measured by the quantitative real-time PCR assay. MC3T3-E1 cells were treated with 1 μ M resveratrol combined with IC182780 or with siER α at the indicated concentrations, and the expression of BMP-2 protein was analyzed by Western blotting. *D*, DNA-binding activity of ER α in resveratrol-treated cells. Nuclear extracts of MC3T3-E1 cells with indicated treatments were isolated and subjected to electrophoretic mobility shift assay analysis as described under "Experimental Procedures." The ER α -specific complex is indicated by an arrow. NRP, non-radiolabeled ER α -binding probe.

ected cells, but not in pBMP2 Δ 2- or pBMP2 Δ 3-transfected cells (Fig. 4A). The pBMP2 Δ 1 promoter is reported to contain an estrogen receptor response element (ERE) and one GC-rich Sp1 response element (15). To ascertain which of these response elements participates in the regulation of BMP-2 promoter activity in response to resveratrol, pBMP2 promoter-reporter mutation constructs containing the mutated ERE and Sp1 response element were used. Resveratrol-induced BMP-2 promoter activity decreased \sim 80% by point mutation of the ERE on pBMP2 (pBMP2/mERE), but this activity was not affected by the pBMP2/mSp1 construct (Fig. 4B). To ascertain whether resveratrol induces the association of the ER with the BMP-2 promoter, a ChIP assay was

employed. Using specific antibodies to various transcription factors, ER α , but not other transcription factors, was found to associate with the BMP-2 promoter after treatment with resveratrol in MC3T3-E1 cells (Fig. 4C). A parallel ChIP experiment was performed to test the specificity of the chromatin association. Sp1 and c-Jun were recruited to their documented targets, the vitamin D3 receptor promoter and the transforming growth factor β 1 promoter (24, 25), respectively (supplemental Fig. S1). By contrast, ER α did not associate with the vitamin D3 receptor promoter or the transforming growth factor β 1 promoter (supplemental Fig. S1).

The quantitative real-time PCR assay was employed to determine the relative concentrations of the ER-DNA complex after

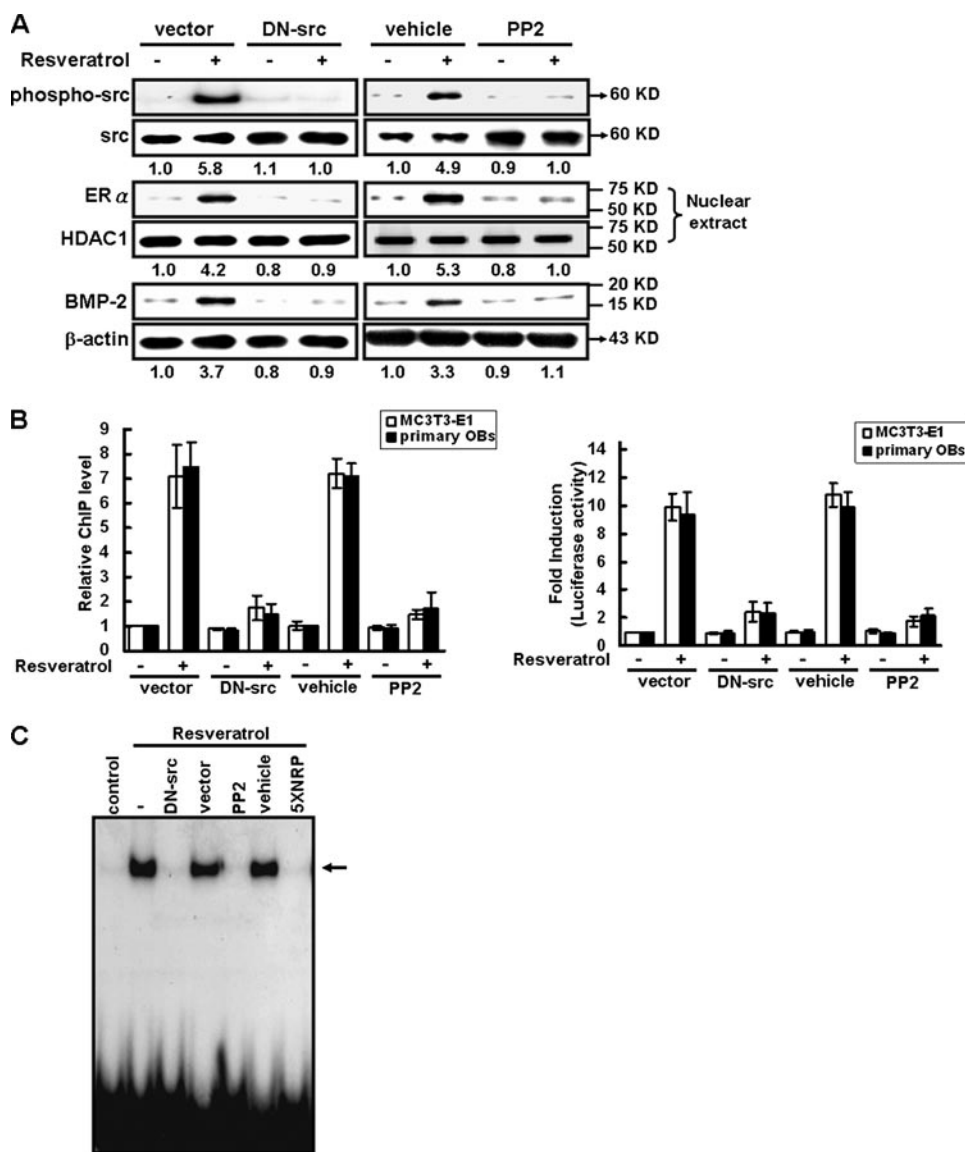


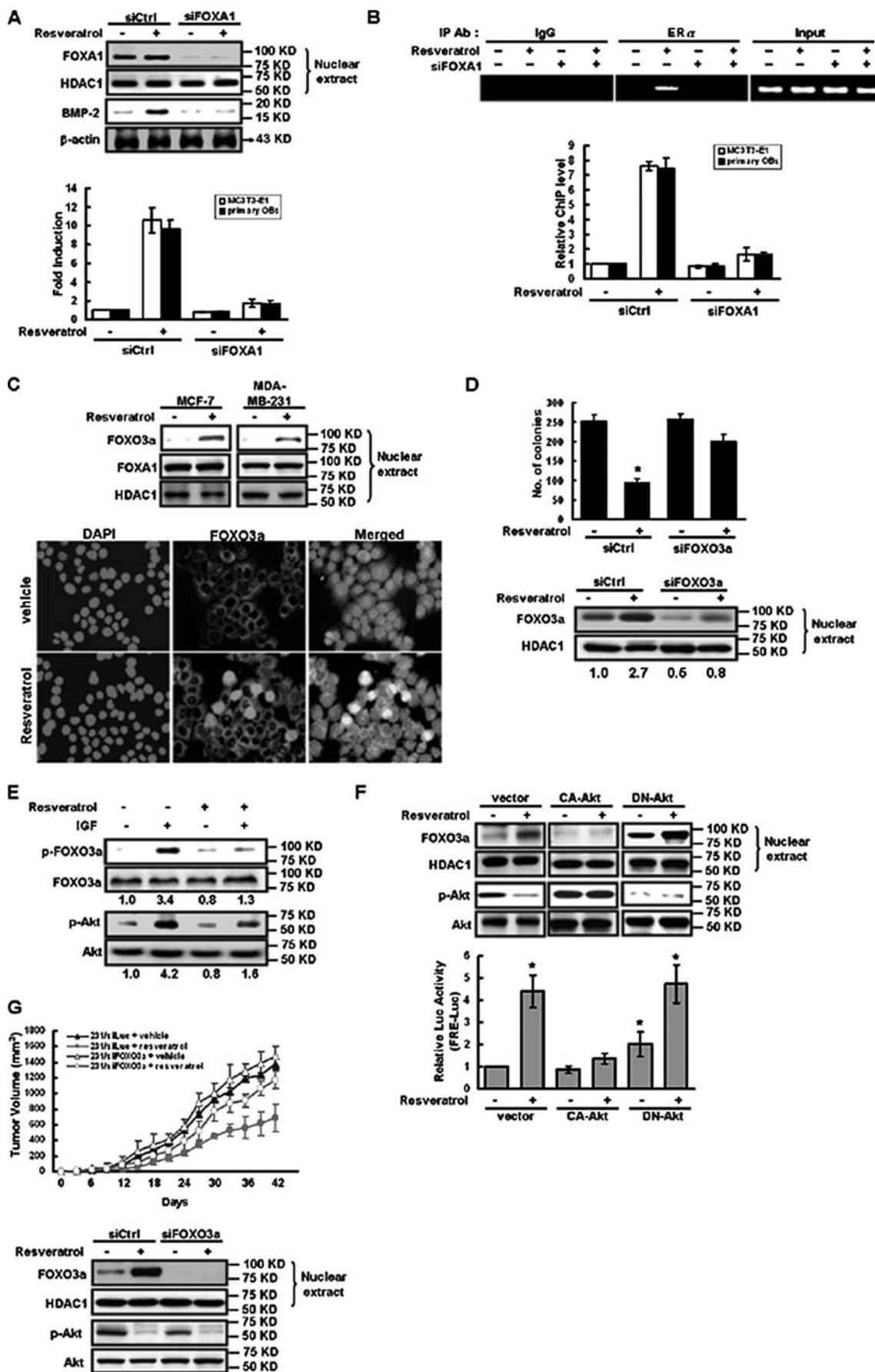
FIGURE 5. Src is required for ER-mediated BMP-2 expression in response to resveratrol. *A*, Src kinase phosphorylation in resveratrol-treated cells. MC3T3-E1 cells were transfected with DN-Src expression vector (3 μ g) or with PP2 (10 μ M) in the presence or absence of resveratrol (1 μ M) and subsequently analyzed for Src phosphorylation, ER α nuclear translocation, and BMP-2 expression by Western blotting. Data are representative of three independent experiments. *B*, involvement of Src kinase in resveratrol-induced ER-DNA complex formation and BMP-2 expression. MC3T3-E1 cells were transfected with DN-Src expression vector (3 μ g) or treated with PP2 (10 μ M) in the presence or absence of resveratrol (1 μ M) and subsequently analyzed for the amount of ER-DNA complex (*left panel*) and BMP-2 promoter activity (*right panel*). Bars indicate means \pm S.D. Values for increases in complex formation or in promoter activity are expressed relative to those for the untreated vector control. *C*, the nuclear extracts of MC3T3-E1 cells with indicated treatments were isolated and subjected to electrophoretic mobility shift assay analysis as described under "Experimental Procedures." The ER α -specific complex is indicated by an arrow. NRP, non-radiolabeled ER α -binding probe.

a ChIP assay. Levels of the resveratrol-induced ER-DNA complex were decreased by treatment with ICI182780 or tamoxifen in a dose-dependent manner (Fig. 4C). Resveratrol-induced BMP-2 expression was also abolished by ER α -specific short interfering RNA (siER α) or ICI182780 (Fig. 4C). Electrophoretic mobility shift assays were subsequently performed to examine the DNA-binding activity of ER α in resveratrol-treated cells. The DNA-binding activity of ER α in nuclear extracts of MC3T3-E1 cells was increased significantly by treatment of these cells with resveratrol (Fig. 4D). However, ER α could not form a DNA complex with mutant ERE probe in

resveratrol-treated cells (Fig. 4D, lane 3). Resveratrol-dependent binding of ER α to DNA was strongly attenuated by specific competition with 5-fold of the non-radiolabeled ER α -binding probe (Fig. 4D, lane 4). This attenuation was not observed, however, when the mutated Sp1 probe was utilized (Fig. 4D, lane 5). The DNA-binding activity of ER α in resveratrol-treated cells was also found to be reduced strongly after treatment with the ER-specific antagonist ICI182780 or with siER α (Fig. 4D). These findings establish that ER α is essential for resveratrol-mediated BMP-2 up-regulation in osteoblasts.

In previous studies in this laboratory, Src kinase was found to serve as a transducer of signaling events occurring in osteoblast cells in response to estrogen-like compounds (26). The involvement of Src kinase in resveratrol-induced ER-dependent BMP-2 expression was therefore of interest. Resveratrol was found to increase the phosphorylation of Src kinase in osteoblastic cells, and this phosphorylation was diminished by transfection with the dominant-negative mutant Src (DN-Src) expression vector or by treatment with the Src kinase inhibitor, PP2 (Fig. 5A). Furthermore, transfection with the DN-Src expression vector or treatment with PP2 significantly decreased resveratrol-induced nuclear translocation of ER α and subsequent BMP-2 expression in MC3T3-E1 cells (Fig. 5A). Experiments were also performed to ascertain whether Src kinase is involved in resveratrol-induced ER-DNA complex formation and BMP-2 expression in

MC3T3-E1 cells and primary OBs. Treatment with resveratrol significantly increased ER-DNA complex formation and pBMP2 luciferase activity in osteoblast cells, and these increases were abolished by transfection with DN-Src expression vector or treatment with PP2 (Fig. 5B). An electrophoretic mobility shift assay was employed to examine the involvement of Src kinase in the resveratrol-induced DNA-binding activity of ER α . As anticipated, the resveratrol-induced DNA-binding activity of ER α was reduced by transfection with DN-Src expression vector or treatment with the chemical inhibitor of Src kinase (Fig. 5C). Taken together, these findings reveal that



Src kinase-mediated ER signaling is required for resveratrol-induced BMP-2 expression.

Forkhead Proteins Play a Unique and Essential Role in Resveratrol-mediated BMP-2 Induction and Tumor Suppression—The pioneer factor, FOXA1, is reported to possess the ability to initiate chromatin opening events (27) and to establish a promoter environment favorable to transcriptional activation by ER α (21, 28). Experiments were therefore performed to determine whether FOXA1 is involved in resveratrol-induced ER-mediated BMP-2 expression. MC3T3-E1 cells were transfected with siRNA for FOXA1 (siFOX1) to target knockdown of FOXA1 protein, followed by measurements of resveratrol-induced BMP-2 expression and pBMP2 luciferase activity. Stably transfected with siFOX1, but not control siRNA (siCtrl), decreased both resveratrol-induced BMP-2 expression and pBMP2 luciferase activity significantly (Fig. 6A). The level of resveratrol-induced ER-DNA complex in osteoblasts was also decreased by siFOX1 (Fig. 6B). These findings suggest FOXA1 plays a critical role in resveratrol-induced ER-mediated BMP-2 expression and subsequent osteogenic response.

Expression and nuclear translocation of forkhead proteins have been shown to mediate apoptosis via activation of proapoptotic genes in a variety of cell types. It was therefore of interest to ascertain whether resveratrol-induced tumor-suppressive effects were exerted through the regulation of forkhead proteins. To this end, Western blotting and immunofluorescence staining experiments were performed. Interestingly, Western blot analysis revealed significant difference of FOXO3a, but not FOXA1, in nuclear fractions of both ER-positive (MCF-7) and ER-negative (MDA-MB-231) breast cancer cells treated with resveratrol but not with vehicle (Fig. 6C). Furthermore, nuclear staining for FOXO3a was consistently observed in resveratrol-treated MDA-MB-231 cells, but not control cells (Fig. 6C). The effects of resveratrol on FOXO3a-dependent transcriptional activation were also examined using a promoter containing the FOXO-responsive elements (FRE) that drive a luciferase (luc) reporter gene. Treatment of MDA-MB-231 breast cancer cells with resveratrol resulted in strong induction of FOXO3a activity, and this induction was abolished in the presence of FOXO3a-specific siRNA (siFOX3a, supplemental Fig. S2). Consistent with these FRE-luc findings, FOXO3a activation

of the p27^{Kip1} and Fas-ligand promoters was also significantly increased by resveratrol (supplemental Fig. S2). To search for additional functional linkages between FOXO3a and resveratrol-mediated tumor suppression, FOXO3a expression in resveratrol-treated cells was subjected to knockdown by siFOXO3a. Fig. 6D reveals that stably expressed cells with siFOXO3a markedly overturned the inhibition by resveratrol of anchorage-independent colony formation of breast cancer cells. These findings substantiate the involvement of FOXO3a in resveratrol-mediated tumor suppression.

The Forkhead factors are direct downstream targets for Akt, and phosphorylation of these factors by Akt has been shown to promote their cytoplasmic retention and inactivation (29). The involvement of Akt in regulation of FOXO3a in response to resveratrol treatment was therefore of interest. Treatment of MCF-7 cells with the resveratrol resulted in inhibition of IGF-induced phosphorylation of FOXO3a at the Thr³² residue, a site known to be phosphorylated by Akt, as well as in phosphorylation of Akt itself (Fig. 6E). More importantly, resveratrol-induced Akt inactivation, FOXO3a nuclear accumulation, and FOXO3a activity were all abolished by transfection with constitutively activated Akt (CA-Akt) and were all enhanced by transfection with dominant negative Akt (DN-Akt) (Fig. 6F). These findings strongly support the proposal that dephosphorylation and, therefore, nuclear accumulation of FOXO3a in response to resveratrol treatment result from Akt inactivation.

It was unclear whether resveratrol-mediated tumor suppression was also the consequence of induction of FOXO3a function. siRNA-mediated gene silencing experiments were therefore performed to down-regulate FOXO3a in MDA-MB-231 cells. Primary tumors of FOXO3a-specific siRNA-treated and control siRNA-treated MDA-MB-231 cells were then developed in nude mice. Consistent with findings described above, treatment with resveratrol decreased Akt activation significantly and induced nuclear accumulation of FOXO3a in primary tumors of control siRNA-treated cells (Fig. 6G). However, a striking rescue by FOXO3a-siRNA of resveratrol-mediated suppression of tumor growth was observed (Fig. 6G), supporting a FOXO3a requirement for resveratrol-induced tumor suppression.

FIGURE 6. Forkhead proteins are essential for resveratrol-mediated BMP-2 induction and tumor suppression. A, effects of FOXA1-siRNA on resveratrol-dependent BMP-2 expression. MC3T3-E1 cells transfected with FOXA1-siRNA (siFOX1) or control siRNA (siCtrl) and treated with or without 1 μ M resveratrol were subjected to Western blot analysis and BMP-2 promoter activity assays. Bars indicate means \pm S.D. B, effect of FOXA1-siRNA on resveratrol-induced ER-DNA complex formation. Osteoblasts were treated with siCtrl or siFOX1 in the presence or absence of 1 μ M resveratrol and then processed for a ChIP assay. Relative levels of ER-DNA complex after the assay were determined by quantitative real-time PCR assay. C, forkhead proteins and resveratrol-induced tumor suppression. Nuclear fractions were prepared from the indicated breast cancer cells treated with or without resveratrol as described under "Experimental Procedures." Nuclear fractions were subjected to Western blot analysis using the indicated antibodies (upper panel). HDAC1 acted as the internal loading control for nuclear fractions. Nuclear accumulation of FOXO3a was observed by fluorescence microscopy (lower panel). The position of MDA-MB-231 cells nucleus was confirmed by staining with Hoechst 33258 fluorescent dye. Findings are representative of three independent experiments. D, effect of FOXO3a-siRNA on resveratrol-inhibited anchorage-independent colony formation. MDA-MB-231 cells transfected with FOXO3a-siRNA (siFOX3a) or control siRNA (siCtrl) and treated with or without resveratrol and were subjected to Western blot analysis and to the soft agar colony-forming assay. Bars indicate means \pm S.D. Asterisks denote a statistically significant induction compared with values of lane 1. E, decreased insulin-like growth factor (IGF)-dependent phosphorylation of Akt and FOXO3a in resveratrol-treated cells. Control or resveratrol-treated MDA-MB-231 cells were treated with or without IGF. Lysates were analyzed by Western blot analysis. F, effects of constitutively activated Akt (CA-Akt) and dominant negative Akt (DN-Akt) on resveratrol-induced Akt inactivation, FOXO3a nuclear accumulation, and FOXO3a activity. MDA-MB-231 cells transfected with vector, CA-Akt, or DN-Akt were treated with or without resveratrol. Preparations were then analyzed by Western blotting and for BMP-2 promoter activity. G, growth patterns, expression of nuclear FOXO3a protein, and phosphorylation of Akt in orthotopic xenograft tumors formed in nude mice by MDA-MB-231 cells transfected with siFOXO3a or siCtrl. Mice were treated with vehicle or resveratrol (10 mg/kg/2 days). Results are presented as means \pm S.D. of eight primary tumors.

DISCUSSION

In the present study, our results provide the evidences to show the phytoestrogen, resveratrol, would be a critical strategy for a therapeutic or preventive intervention for bone loss without increase the breast cancer risk through the regulation of forkhead proteins. It was conceivable that other events, such as down-regulation of BMP-3, contributed to the resveratrol-induced osteogenic response. BMP-3 is reported to serve as an antagonist of osteogenic BMPs (30). In the present study resveratrol was found by microarray analysis to decrease the expression of BMP-3 mRNA; this observation was confirmed by RT-PCR (supplemental Table S1 and Fig. 3A). Furthermore, treatment with recombinant BMP-3 modestly decreased the resveratrol-induced osteogenic response in C2C12 cells (data not shown). These findings support the proposal that resveratrol exerts its bone-protective effects through induction of osteogenic BMP-2 and through reduction of anti-osteogenic BMP-3. The osteogenic activity of resveratrol, similarly to that of osteogenic drugs such as parathyroid hormone, is associated with increased BMD, with improved bone structure, and with a decreased risk of vertebral and non-vertebral fractures (31). Inhibition of bone resorption is a separate approach in treatment of osteoporosis, and the objective of most current pharmacological therapies for osteoporosis is to inhibit excessive bone resorption (32). Resveratrol is reported to prevent osteoclast differentiation by interference with receptor activator of NF- κ B signaling (6). Resveratrol was found⁴ to inhibit macrophage-colony stimulating factor and receptor activator of NF- κ B-induced osteoclast differentiation. The mechanism responsible for the inhibition, however, was not explored.

We have found that resveratrol is a stimulant for *BMP-2* gene expression in osteoblast cells, and the stimulation of osteoblast differentiation by resveratrol is BMP-dependent (Fig. 3). These results explain that the effect of resveratrol in prevention of bone loss in OVX rats, which we have confirmed, is mediated by BMP-2. BMP-2 is an autocrine and paracrine growth factor and is expressed from early stages of embryonic development and in adulthood, primarily in bone-forming tissues (33). During osteoblastic differentiation, *BMP-2* mRNA is induced, and maintains the sustained phenotype of mature osteoblasts (33). Previous studies have indicated that the *BMP-2* gene regulation during limb morphogenesis and osteoblast differentiation may involve multiple mechanisms and signaling pathways, such as ER, prostaglandin E₂, retinoic acid, Hoxa13, Gli2/3, interferon, and interleukins (34–36). Resveratrol has been found to be an agonist for the ERs that are required for osteogenic differentiation (3). The studies on mouse bone marrow mesenchymal stem cells have shown that the resveratrol promotes osteoblastic differentiation through the ER/NO/cGMP pathway (37). As we indicated in Fig. 3, the mouse *BMP-2* promoter contains ER response elements. Our data on *BMP-2* promoter analyses suggest that the enhancement of BMP-2 transcription induced by resveratrol is mediated by ER through its binding sites in the promoter. These results are consistent with the findings that estrogens activate BMP-2 transcription, which requires ER α

and ER β acting via a variant estrogen-responsive element binding sites in the promoter, with ER α being the more efficacious regulator (37). Coincidentally, the animal studies have shown that systemic intra-peritoneal injection of rhBMP-2 rescues the bone loss in estrogen-deficient mice (38). Thus, the stimulation of the ER/BMP-2 pathway in osteogenic cells is a mechanism by which resveratrol exerts its anabolic function in bone.

Resveratrol is an anti-aging compound. Recent aging studies reported that the effect of resveratrol to increase lifespan is mediated through an SIRT1-dependent pathway (39, 40). SIRT1 is an NAD⁺-dependent deacetylase and an ortholog of yeast deacetylase Sir2 (silent information regulator). Small molecule compound screening has found that resveratrol is a potent activator of SIRT1 with the highest activity to lower the K_m for the acetylated substrate of SIRT1. Resveratrol also enhances *SIRT1* gene expression (39, 40). It was reported that Foxo3a, a forkhead transcription factor, plays a direct role in mediating *SIRT1* transcription, through two p53 binding sites present in the *SIRT1* promoter (41). In our present study, we found that resveratrol increases Foxo3a activity in cancer cells, and expression and resveratrol enhancement of BMP-2 expression are FoxA1-dependent (Fig. 6). The combined data indicate that Forkhead proteins are targets of resveratrol in osteoblasts. Resveratrol was also found to enhance expression and activity of endothelial nitric-oxide synthase and nitric oxide production (37). In endothelial nitric-oxide synthase knock-out mice, both SIRT1 expression and bone mass are reduced (42). These results suggest that the endothelial nitric-oxide synthase/nitric oxide pathway is one of the mechanisms by which resveratrol enhances SIRT1 expression in bone.

Multiple cellular functions, including cell cycle arrest, DNA repair, detoxification, cell differentiation, cell death, atrophy, glucose metabolism, and angiogenesis are thought to be regulated by forkhead proteins (43, 44). However, the role of forkhead proteins in bone development is largely unknown. FOXC1 and FOXC2 are reported to be regulated by BMP-2 and to be required for BMP-2-induced osteoblastic differentiation (45). The present report is therefore the first to reveal that FOXA1 is required for an ER-mediated osteogenic response.

IKK is reported to promote tumorigenesis through induction of ubiquitination-dependent degradation of FOXO3a (22). Findings from this laboratory⁴ and of others (46) reveal that resveratrol is an inhibitor of IKK activity. Whether resveratrol also increases FOXO3a stability via inactivation of IKK requires further investigation. IKK is known to be critical to osteoclast survival and differentiation and to inflammation-induced bone loss (47). It is therefore conceivable that inactivation of IKK is essential to resveratrol-induced osteoclast differentiation and to the anti-resorptive effects of this agent.

In this study, we found ER plays the critical role in resveratrol-mediated BMP-2 expression in osteoblast cells (Fig. 4), however, we also found resveratrol-induced tumor-suppressive effects in ER-positive and ER-negative breast cancer cells (Fig. 4). These data indicated that resveratrol-induced anti-tumor activity may occur through ER-independent pathways (Fig. 4). Tumor suppression may be caused by multiple events, including the inactivation of oncogenes and activation of specific tumor suppressor genes (48). It has

⁴ J.-L. Su, C.-Y. Yang, M. Zhao, M.-L. Kuo, and M.-L. Yen, unpublished findings.

been reported that resveratrol-induced tumor-suppressive effects are associated with inactivation of Akt (49, 50), a critical kinase for survival signaling in both ER-positive and ER-negative breast cancer cells (51). Our data, consistent with others', also showed that resveratrol significantly inhibits Akt activity and further increases the tumor suppressor, FOXO3a, in both ER-positive (MCF-7) and ER-negative (MDA-MB-231) breast cancer cells (Fig. 6). These data suggest that resveratrol-induced inactivation of Akt and induction of FOXO3a may be one of the mechanisms involved in resveratrol-mediated similar anti-tumor effects on ER-positive and ER-negative breast cancer cells.

In conclusion, the phytoestrogen, resveratrol, exerts its bone-sparing and tumor-suppressive actions through regulation of specific forkhead proteins. The findings of this report support the use of resveratrol as a critical strategy for therapeutic or preventive intervention for bone loss. Resveratrol is as effective as estrogen for maintaining bone density, but, unlike estrogen, is not associated with an increased risk of breast cancer.

Acknowledgments—We thank Dr. Ching-Chow Chen (Dept. of Pharmacology, College of Medicine, National Taiwan University, Taipei, Taiwan) for providing the DN-Akt plasmid and Dr. Ruey-Hwa Chen (Dept. of Molecular Medicine, College of Medicine, National Taiwan University, Taipei, Taiwan) for providing the dominant-negative mutant Src plasmid. We also thank Dr. Mien-Chie Hung (Dept. of Molecular and Cellular Oncology, The University of Texas, M. D. Anderson Cancer Center) for providing promoter reporters and helpful discussion.

REFERENCES

- Mundy, G. R. (2006) *Am. J. Clin. Nutr.* **83**, 427S–430S
- Couzin, J. (2003) *Science* **302**, 1136–1138
- Gehm, B. D., McAndrews, J. M., Chien, P. Y., and Jameson, J. L. (1997) *Proc. Natl. Acad. Sci. U. S. A.* **94**, 14138–14143
- Jang, M., Cai, L., Udeani, G. O., Slowing, K. V., Thomas, C. F., Beecher, C. W., Fong, H. H., Farnsworth, N. R., Kinghorn, A. D., Mehta, R. G., Moon, R. C., and Pezzuto, J. M. (1997) *Science* **275**, 218–220
- Ray, P. S., Maulik, G., Cordis, G. A., Bertelli, A. A., Bertelli, A., and Das, D. K. (1999) *Free Radic. Biol. Med.* **27**, 160–169
- Boissy, P., Andersen, T. L., Abdallah, B. M., Kassem, M., Plesner, T., and Delaisse, J. M. (2005) *Cancer Res.* **65**, 9943–9952
- de la Lastra, C. A., and Villegas, I. (2005) *Mol. Nutr. Food Res.* **49**, 405–430
- Delmas, D., Jannin, B., and Latruffe, N. (2005) *Mol. Nutr. Food Res.* **49**, 377–395
- Su, J. L., Lin, M. T., Hong, C. C., Chang, C. C., Shiah, S. G., Wu, C. W., Chen, S. T., Chau, Y. P., and Kuo, M. L. (2005) *Carcinogenesis* **26**, 1–10
- Delmas, D., Lancon, A., Colin, D., Jannin, B., and Latruffe, N. (2006) *Curr. Drug Targets* **7**, 423–442
- Mizutani, K., Ikeda, K., Kawai, Y., and Yamori, Y. (2000) *J. Nutr. Sci. Vitaminol. (Tokyo)* **46**, 78–83
- Andreou, V., D'Addario, M., Zohar, R., Sukhu, B., Casper, R. F., Ellen, R. P., and Tenenbaum, H. C. (2004) *J. Periodontol.* **75**, 939–948
- Massague, J. (1998) *Annu. Rev. Biochem.* **67**, 753–791
- Wozney, J. M., Rosen, V., Celeste, A. J., Mitscock, L. M., Whitters, M. J., Kriz, R. W., Hewick, R. M., and Wang, E. A. (1988) *Science* **242**, 1528–1534
- Zhao, M., Harris, S. E., Horn, D., Geng, Z., Nishimura, R., Mundy, G. R., and Chen, D. (2002) *J. Cell Biol.* **157**, 1049–1060
- Fleet, J. C., Cashman, K., Cox, K., and Rosen, V. (1996) *Endocrinology* **137**, 4605–4610
- Matsumoto, A., Yamaji, K., Kawanami, M., and Kato, H. (2001) *J. Periodontol. Res.* **36**, 175–182
- Styrkarsdottir, U., Cazier, J. B., Kong, A., Rolfsson, O., Larsen, H., Bjarnadottir, E., Johannsdottir, V. D., Sigurdardottir, M. S., Bagger, Y., Christiansen, C., Reynisdottir, I., Grant, S. F., Jonasson, K., Frigge, M. L., Gulcher, J. R., Sigurdsson, G., and Stefansson, K. (2003) *PLoS Biol.* **1**, E69
- Su, J. L., Yang, P. C., Shih, J. Y., Yang, C. Y., Wei, L. H., Hsieh, C. Y., Chou, C. H., Jeng, Y. M., Wang, M. Y., Chang, K. J., Hung, M. C., and Kuo, M. L. (2006) *Cancer Cell* **9**, 209–223
- van der Horst, G., van Bezooijen, R. L., Deckers, M. M., Hoogendam, J., Visser, A., Lowik, C. W., and Karperien, M. (2002) *Bone* **31**, 661–669
- Carroll, J. S., Liu, X. S., Brodsky, A. S., Li, W., Meyer, C. A., Szary, A. J., Eeckhoutte, J., Shao, W., Hestermann, E. V., Geistlinger, T. R., Fox, E. A., Silver, P. A., and Brown, M. (2005) *Cell* **122**, 33–43
- Hu, M. C., Lee, D. F., Xia, W., Golfman, L. S., Ou-Yang, F., Yang, J. Y., Zou, Y., Bao, S., Hanada, N., Saso, H., Kobayashi, R., and Hung, M. C. (2004) *Cell* **117**, 225–237
- Zhou, S., Turgeman, G., Harris, S. E., Leitman, D. C., Komm, B. S., Bodine, P. V., and Gazit, D. (2003) *Mol. Endocrinol.* **17**, 56–66
- Kim, S. J., Angel, P., Lafyatis, R., Hattori, K., Kim, K. Y., Sporn, M. B., Karin, M., and Roberts, A. B. (1990) *Mol. Cell Biol.* **10**, 1492–1497
- Wietzke, J. A., Ward, E. C., Schneider, J., and Welsh, J. (2005) *Mol. Cell. Endocrinol.* **230**, 59–68
- Yen, M. L., Su, J. L., Chien, C. L., Tseng, K. W., Yang, C. Y., Chen, W. F., Chang, C. C., and Kuo, M. L. (2005) *Mol. Pharmacol.* **68**, 1061–1073
- Cirillo, L. A., Lin, F. R., Cuesta, I., Friedman, D., Jarnik, M., and Zaret, K. S. (2002) *Mol. Cell* **9**, 279–289
- Laganier, J., Deblouis, G., Lefebvre, C., Bataille, A. R., Robert, F., and Giguere, V. (2005) *Proc. Natl. Acad. Sci. U. S. A.* **102**, 11651–11656
- Brunet, A., Bonni, A., Zigmond, M. J., Lin, M. Z., Juo, P., Hu, L. S., Anderson, M. J., Arden, K. C., Blenis, J., and Greenberg, M. E. (1999) *Cell* **96**, 857–868
- Daluiski, A., Engstrand, T., Bahamonde, M. E., Gamer, L. W., Agius, E., Stevenson, S. L., Cox, K., Rosen, V., and Lyons, K. M. (2001) *Nat. Genet.* **27**, 84–88
- Neer, R. M., Arnaud, C. D., Zanchetta, J. R., Prince, R., Gaich, G. A., Reginster, J. Y., Hodsmann, A. B., Eriksen, E. F., Ish-Shalom, S., Genant, H. K., Wang, O., and Mitlak, B. H. (2001) *N. Engl. J. Med.* **344**, 1434–1441
- Delmas, P. D. (2002) *Lancet* **359**, 2018–2026
- Anderson, H. C., Hodges, P. T., Aguilera, X. M., Missana, L., and Moylan, P. E. (2000) *J. Histochem. Cytochem.* **48**, 1493–1502
- Garrett, I. R., Chen, D., Gutierrez, G., Zhao, M., Escobedo, A., Rossini, G., Harris, S. E., Gallwitz, W., Kim, K. B., Hu, S., Crews, C. M., and Mundy, G. R. (2003) *J. Clin. Invest.* **111**, 1771–1782
- Abrams, K. L., Xu, J., Nativelle-Serpentini, C., Dabirshahsahebi, S., and Rogers, M. B. (2004) *J. Biol. Chem.* **279**, 15916–15928
- Zhao, M., Qiao, M., Harris, S. E., Chen, D., Oyajobi, B. O., and Mundy, G. R. (2006) *Mol. Cell Biol.* **26**, 6197–6208
- Song, L. H., Pan, W., Yu, Y. H., Quarles, L. D., Zhou, H. H., and Xiao, Z. S. (2006) *Toxicol. in Vitro* **20**, 915–922
- Turgeman, G., Zilberman, Y., Zhou, S., Kelly, P., Moutsatsos, I. K., Kharode, Y. P., Borella, L. E., Bex, F. J., Komm, B. S., Bodine, P. V., and Gazit, D. (2002) *J. Cell. Biochem.* **86**, 461–474
- Howitz, K. T., Bitterman, K. J., Cohen, H. Y., Lamming, D. W., Lavu, S., Wood, J. G., Zipkin, R. E., Chung, P., Kisilewski, A., Zhang, L. L., Scherer, B., and Sinclair, D. A. (2003) *Nature* **425**, 191–196
- Denu, J. M. (2005) *Curr. Opin. Chem. Biol.* **9**, 431–440
- Nemoto, S., Fergusson, M. M., and Finkel, T. (2004) *Science* **306**, 2105–2108
- Nisoli, E., Tonello, C., Cardile, A., Cozzi, V., Bracale, R., Tedesco, L., Falcone, S., Valerio, A., Cantoni, O., Clementi, E., Moncada, S., and Carruba, M. O. (2005) *Science* **310**, 314–317
- Burgering, B. M., and Kops, G. J. (2002) *Trends Biochem. Sci.* **27**, 352–360
- Lehmann, O. J., Sowden, J. C., Carlsson, P., Jordan, T., and Bhattacharya, S. S. (2003) *Trends Genet.* **19**, 339–344
- Rice, R., Rice, D. P., and Thesleff, I. (2005) *Dev. Dyn.* **233**, 847–852

Forkhead Is Critical for BMP-2 and Tumor Suppression

46. Kundu, J. K., Shin, Y. K., Kim, S. H., and Surh, Y. J. (2006) *Carcinogenesis* **27**, 1465–1474
47. Ruocco, M. G., Maeda, S., Park, J. M., Lawrence, T., Hsu, L. C., Cao, Y., Schett, G., Wagner, E. F., and Karin, M. (2005) *J. Exp. Med.* **201**, 1677–1687
48. Dillon, R. L., White, D. E., and Muller, W. J. (2007) *Oncogene* **26**, 1338–1345
49. Li, Y., Liu, J., Liu, X., Xing, K., Wang, Y., Li, F., and Yao, L. (2006) *Appl. Biochem. Biotechnol.* **135**, 181–192
50. Aziz, M. H., Nihal, M., Fu, V. X., Jarrard, D. F., and Ahmad, N. (2006) *Mol. Cancer Ther.* **5**, 1335–1341
51. Kumar, R., and Hung, M. C. (2005) *Cancer Res.* **65**, 2511–2515

